Max-Planck-Institut für Meteorologie

REPORT No. 326

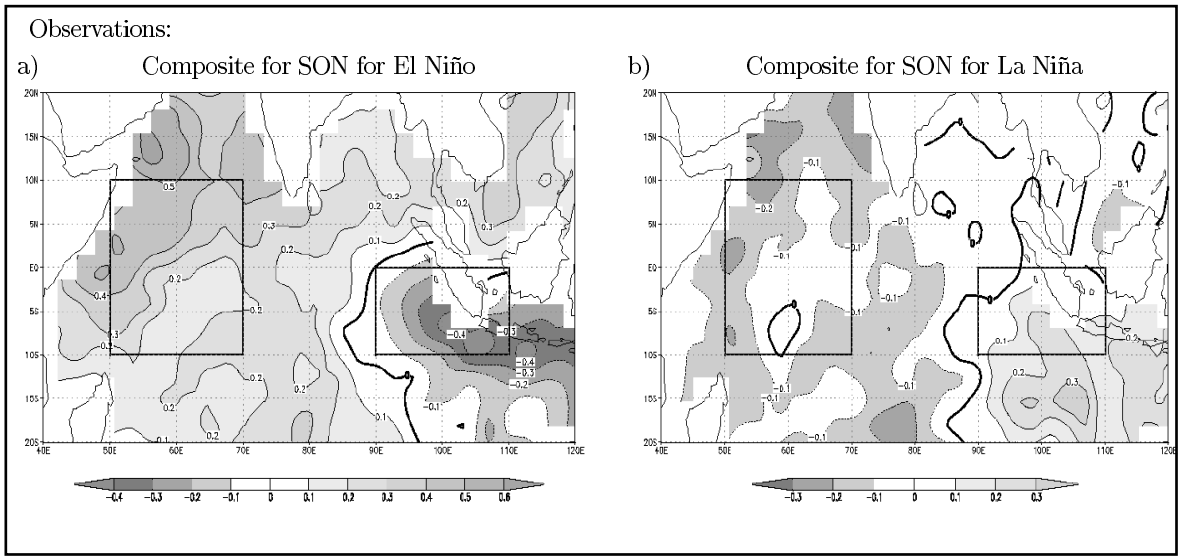

ON DIPOLE-LIKE VARIABILITY IN THE TROPICAL INDIAN OCEAN

by

Astrid Baquero-Bernal and Mojib Latif

HAMBURG, August 2001

AUTHORS:

Astrid Baquero-Bernal, Mojib Latif — Max-Planck-Institut für Meteorologie Hamburg, Germany

MAX-PLANCK-INSTITUT
FÜR METEOROLOGIE
BUNDESSTRASSE 55
D-20146 HAMBURG
F.R. GERMANY

Tel.: +49 - (0)40 - 411 73 - 0
Telefax: +49 - (0)40 - 411 73 - 298
E-Mail: <name>@dkrz.de

On dipole-like variability in the tropical Indian Ocean

Astrid Baquero-Bernal and Mojib Latif
Max-Planck Institut für Meteorologie, Hamburg

E-mail: baquero@dkrz.de
latif@dkrz.de

Submitted to Journal of Climate

ISSN 0937-1060

Abstract

The interannual variability of the tropical Indian Ocean sea surface temperature (SST) is studied with observational data and a hierarchy of coupled general circulation models (CGCMs). Special attention is given to the question whether an oscillatory dipole mode exists in the tropical Indian Ocean region with centers east and west of 80°E. Our observational analyses indicate that dipole-like variability can be explained as an oscillatory mode only in the context of ENSO (El Niño/Southern Oscillation).

A dipole-like structure in the SST anomalies independent of ENSO was found also. Our series of coupled model experiments shows that ocean dynamics is not important to this type of dipole-like SST variability. It is forced by surface heat flux anomalies that are integrated by the thermal inertia of the oceanic mixed layer, which reddens the SST spectrum.

1 Introduction

Since the interannual variability in the tropical Indian Ocean sea surface temperature (SST) is much weaker than that in the Pacific, it did not receive so much attention and is less well understood than the variability in the Pacific. The latter is dominated by the El Niño/Southern Oscillation (ENSO) phenomenon. Although ENSO originates in the tropical Pacific, it affects the global climate. Several investigations have suggested that ENSO also influences the Indian Ocean in different ways (Latif and Barnett, 1995; Tourre and White, 1997; Chambers et al., 1999; Venzke et al., 2000; Meyers, 1996). Other studies have suggested that a significant fraction of the SST variability is related to ENSO but that there are other factors that are also important in determining the SST anomalies (SSTA) (Reverdin et. al, 1986: Murtugudde, 1999). Recently, Saji et al. (1999) and Webster et al. (1999) have proposed the existence of a coupled ocean-atmosphere mode that originates in the Indian Ocean climate system, which has characteristic seasonal phase locking and may induce anomalous rainfall over eastern Africa and Indonesia. Furthermore, it is argued that the mode is independent of ENSO. The mode is referred to as the "Dipole Mode (DM)". The DM spatial structure they proposed is characterized by SSTAs of one sign in the southeastern tropical Indian Ocean (SETIO: 90°E - 110°E, 10°S - 0°) and SSTAs of the opposite sign in the western tropical Indian Ocean (WTIO: 50°E - 70°E, 10°S - 10°N).

Here we investigate the interannual variability in the tropical Indian Ocean SST and its relationship to ENSO in more detail. SST observations and results from a series of coupled model integrations are used. We apply correlation analyses using area-averaged anomalies and the technique of Principal Oscillation Patterns (POPs) to remove the ENSO signal. POP analysis is designed to extract the characteristic space-time variations within a complex multi-dimensional system (Hasselmann, 1988; von Storch et al.,

1988; Xu and von Storch, 1990). We show that an oscillatory dipole-like structure like the one proposed by Saji et al. (1999) exists only as part of the ENSO cycle. There exists, however, dipole-like variability in the Indian Ocean independent of ENSO, but this type of variability is driven by the atmosphere.

The paper is organized as follows. The results of the analyses of the observed SSTs are presented in the section 2. We describe the results of the coupled model simulations in section 3. We present our major conclusions in section 4.

2 SST observations

We use the monthly SST dataset from the Hadley Center for Climate Prediction and Research (Folland et al. 1999). Although the dataset covers the period 1870- 1998, we analyzed only the period 1949 to 1998 which is commonly believed to be the most reliable period. The SSTAs were calculated by subtracting the mean annual cycle. We consider the region 40°E to 60°W and 30°S to 30°N, which corresponds to the tropical Indian and Pacific Oceans. To perform the correlations between global and box-averaged SSTAs we always used mean seasonal values. We also performed a POP analysis based on monthly values in order to identify the ENSO-related SST variability and to remove it from the full dataset.

2.1 Analysis considering all the seasons

The correlations of the Indo-Pacific SSTAs with box averaged SSTAs in SETIO and WTIO are shown in Fig. 1. The WTIO box shows significant correlations with equatorial SSTAs in the Pacific Ocean, but it has no negative correlation with the anomalies in SETIO (Fig. 1a). The SETIO box does not show either any significant positive or negative correlation with the SSTAs in

WTIO, and the correlations with the SSTAs in the Pacific are smaller. Both correlation maps (Fig. 1a and 1b) lead to the conclusion that the SSTAs in SETIO and in WTIO are not significantly negatively correlated with each other at lag zero, which is consistent with the results of Dommenget and Latif (2001). Additionally, we performed lagged cross-correlation analyses between the SSTAs in SETIO and those in WTIO. We found that maximum cross-correlation (r=0.43) occurs when the SST variations in SETIO lag those in WTIO by 1 season. Higher correlations are found when the cross-correlation analysis is performed with respect to the Niño3 time series. We found maximum cross-correlation (r=0.65) when the SSTAs in the western Indian Ocean lag those of the eastern Pacific by about 1 season, which is consistent with the results of Venzke et al. (2000). Maximum cross correlation (r=0.48) is obtained when the SSTAs in the eastern Indian Ocean lag those of the eastern Pacific by 2 seasons. This lag of 2 seasons is consistent with the fact that the SSTAs in SETIO lag those in WTIO by 1 season. At lag zero, the correlation between WTIO and Niño3 time series is positive and close to the maximum value of about 0.60. It should be noted that although the maximum correlation between the SSTAs in SETIO and Niño3 is at lag=1 season, the correlation at lag zero is also positive and relatively strong.

In summary, the results of the correlation analyses and the cross-correlation analyses with respect to the SSTA in the eastern Pacific (Niño3) reveal that the SST variability in the Indian Ocean is strongly remotely forced by the ENSO phenomenon. Furthermore, a dipole-like mode cannot be identified if all seasons are considered.

2.2 Seasonal analyses

In the next step, we computed the correlation maps for every season separately (like those shown in Fig. 1). No negative correlation was found between the SSTAs in SETIO and WTIO neither in winter nor in spring (not shown).

For the boreal summer season, there is a very weak negative correlation between the SSTAs in the WTIO and those near the western coast of Indonesia and the north-western coast of Australia (not shown). Some stronger cross Indian Ocean gradient, however, was found in boreal fall. More importantly, this is the season when a strong correlation between the surface westerlies over the equatorial Indian Ocean and the rainfall at the coast of East Africa can be found (Hastenrath et al, 1993). Accordingly, the boreal fall season (SON) will be considered in detail.

2.3 Analysis for SON

We turn now to the boreal fall season. The SSTAs in WTIO show negative correlations with those in the eastern Indian Ocean, but they are restricted to a small region (Fig. 2a). The SETIO SSTAs do show negative correlations with those in the central Indian region, which are strongest south of the equator (Fig. 2b). Both correlation maps, however, show that the SSTAs in SETIO and in WTIO are not strongly negatively correlated with each other. Furthermore, the SSTAs in the two boxes, SETIO and WTIO, are strongly correlated with the SSTAs in the Pacific. This contradicts the claim of Saji et al. (1999) that there exists an ENSO-independent dipole mode, with centers of action in WTIO and SETIO.

Fig. 3 shows the composites for El Niño and La Niña events. Fig. 3a shows the composite for the six recent El Niño events (1957, 1965, 1972, 1982, 1987 and 1997) and Fig. 3b that for the seven recent La Niña events (1955, 1970, 1971, 1973, 1975, 1985 and 1988). ENSO-related variability in the Indian Ocean in the boreal fall season looks like a seesaw: for the El Niño events, there are positive SST anomalies in the western region and negative anomalies in the east. The situation is reversed during La Niña conditions, but the magnitude of the anomalies is smaller in the western region. Figs. 2 and 3 demonstrate clearly that the dipole-like variability in the tropical Indian Ocean is not independent of the ENSO phenomenon.

2.4 ENSO-removed analyses

Our analyses may be influenced by the presence of the strong ENSO signal. We therefore repeated the correlation analyses by removing the ENSO signal prior to the analyses. There is no unique way to do this. Here we subtracted the leading POP mode from the monthly SSTA. Seasonal mean values were then computed from the residual dataset.

The POP analysis of the monthly SSTAs revealed one dominant POP pair (the ENSO mode, not shown) accounting for 26.4% of the total variance. The rotation period of this POP pair amounts to 42 months, with a decay time of 10 months. All other POPs were statistically insignificant. The dominant POP pair is clearly associated with ENSO, which can be inferred from the correlation of the complex coefficient time series (not shown) with the Niño3 (5°S - 5N, 150°W -90°W) SSTA time series. The zero lag correlation of the real part time series with the Niño3 time series amounts to 0.94 and the 4-months lag correlation of the imaginary part time series with the Niño3 time series to 0.74. A cross spectral analysis of the two coefficient time series (not shown) showed the theoretically expected result that they are highly coherent (above the 99% significance level) with a phase shift of about -90° for periods between 20 and 70 months.

2.4.1 Analysis considering all the seasons

The correlations of the Indo-Pacific SSTAs with the averaged SSTAs in SETIO and WTIO based on seasonal values are shown in Fig. 4. Again (as shown in Fig. 1 by retaining the full data set), the correlation maps obtained from the "ENSO-removed" data show that the SSTA in the eastern and western parts of the Indian Ocean are not significantly correlated with each other, when we consider all 4 seasons together.

2.4.2 Analysis for SON

Fig. 5 shows the correlations of the Indo-Pacific SSTAs with box averaged SSTAs in SETIO and WTIO for the fall season. A negative correlation between the SSTAs in SETIO and those in the central (but not western) Indian Ocean is seen in Fig. 5b. These negative correlations are larger than those in Fig. 2b and they extend to the north of the equator. In conclusion, Figs. 2, 4 and 5 show that SSTAs in the eastern and western parts of the Indian Ocean are not strongly negatively correlated, and that there is a significant negative correlation between the SSTAs in the eastern and central parts of the Indian Ocean during the boreal fall season. This anti-correlation between the eastern and central regions exists also when the ENSO signal is removed from the data. In the next section we shall discuss the mechanisms that may explain this dipole-like variability by analyzing a suite of coupled model simulations.

3 Coupled model simulations

We turn now to the coupled model simulations. We analyzed three different coupled model runs. The first coupled run is an extended range integration with a coupled ocean-atmosphere general circulation model (GCM). This run serves as a control integration. The second coupled run is a similar run, but with the ENSO variability suppressed. The ocean GCM is replaced by a fixed-depth mixed layer model in the third coupled run. This set of coupled experiments enables us to investigate the roles of ENSO and ocean dynamics in the generation of the interannual SST variability of the tropical Indian Ocean.

3.1 Fully coupled ocean-atmosphere GCM

To examine the interannual variability independent of ENSO, the subtraction of the leading POP pair may not be the best method. We therefore analyzed additionally the outputs of two simulations with the ECHO-G model (Legutke and Voss (1999)). The ECHO-G model has a horizontal resolution of 2.8 °x 2.8 °. The ocean component uses a higher meridional resolution of 0.5 °within the region 10°N - 10°S. Here we use the first 100 years from the control run, while the coupled run in which the ENSO variability has been suppressed (no-ENSO run) has a duration of 40 years. The suppression of ENSO variability was realized in the coupled model by replacing the actual SSTs simulated by the ocean component in the tropical Pacific by climatology before passing them to the atmosphere model.

Fig. 6 shows the SSTA-correlation maps with the box averaged SST anomalies in the SETIO and in WTIO regions when all seasons are considered. Both simulations, the control run (Fig. 6a and 6b) and the no-ENSO run (Figs. 6c and 6d), show positive correlations almost everywhere in the Indian Ocean. In particular, as in the observations, there is no negative correlation simulated in the two coupled runs between the western and eastern Indian Ocean. These model results confirm our observational results. We conclude further that our results do not depend on the way of subtracting the ENSO signal.

Fig. 7 shows the spectra of box-averaged SST anomalies in the SETIO and WTIO regions for the control and no-ENSO runs. Each spectrum is tested against the hypothesis that the spectrum is produced by a first order autoregressive process (red noise spectrum) and a 95% confidence level for accepting the red noise hypothesis is also shown. For the control run, the spectra of the two boxes (Figs. 7a and 7b) show enhanced variability for periods of 5-10 seasons, i. e. about 1-3 years (the coupled model simulates a quasi-biennial ENSO period). In contrast, the spectra of the no-ENSO run (Figs. 7c and 7d) are consistent with red noise spectra. This result indicates

also that a dipole mode that is associated with a specific timescale does not exist.

The correlation maps for fall (SON) are shown in Fig. 8. Both the control run and the no-ENSO run yield similar correlation maps, with some indication of dipole-like variability. This means that although ENSO was removed physically in the no-ENSO run, there is still a mechanism which produces a dipole-like structure in the SST anomalies in the boreal fall season. The correlation maps for the other seasons (not shown) do not exhibit a dipole-like structure.

3.2 AGCM coupled to a mixed layer ocean

Is the dipole-like variability in the no-ENSO run a result of ocean dynamics or of atmospheric forcing? In order to answer this question, we coupled a mixed layer ocean model with the ECHAM4 atmosphere model (the same atmosphere model that has been used in the coupled runs discussed above). The mixed layer model has a constant depth of 50m and does not carry by definition any ocean dynamics. Variations in the surface heat flux is the only mechanism which can produce SST anomalies in such a model.

Correlation analyses of SST anomalies from the mixed layer simulation are shown in Figs. 9 and 10. Fig. 9 corresponds to the case when all the seasons are considered and Fig. 10 when only fall (SON) is considered. Both Fig. 9 and Fig. 10 show some correspondence with the maps derived from the observations (Figs. 1 and 2), and with those for the coupled runs (Figs. 6 and 8). The spectra of the SST anomalies in the boxes SETIO and WTIO considering all the seasons are consistent with the red noise assumption (not shown). It can be concluded from the results of the mixed layer simulation that an ENSO-independent dipole-like SST anomaly pattern exists in the boreal fall season, which can be explained by atmospheric forcing. Dynamical processes in the ocean are not necessary to produce this type of bipolar SST variability.

4 Conclusions

Correlation analyses of seasonal SST anomalies from the Hadley Center SST observations during the period 1949-1998 and from three different coupled GCM runs show consistent results. The dominant SST variability in the tropical Indian Ocean is related to ENSO. The ENSO-related SST response of the Indian Ocean in the fall season is a dipole. However, we do not find evidence for an ENSO-independent oscillatory mode with dipole-like SST anomalies. Yet, dipole-like variability exists in the tropical Ocean, but this type of variability is driven by the atmosphere and does not involve ocean dynamics.

Most studies so far described the ENSO response in the Indian Ocean as a homogeneous response: During El Niño events, the Indian Ocean exhibits basin wide warm SST anomalies and during La Niña conditions, the SST anomalies are of opposite sign. This is true for some seasons, especially for the winter season (DJF), but for fall (SON), this is generally not the case. We found that in the boreal fall season, on average, the ENSO signal can be seen as a dipole-like pattern: During El Niño events, cold anomalies are observed east of 80°E and warm SST anomalies west of 80°E, during La Niña events, we observe the reverse SST anomaly pattern.

An oscillatory ENSO-independent dipole mode does not exist in the tropical Indian Ocean. This has been validated by simulations with a hierarchy of coupled models. The only mode-like dipole variability (in the physical sense that air-sea interactions lead to an oscillation) is associated with the ENSO phenomenon.

In summary, there is dipole-like variability in the SST of the Indian Ocean. This variability, however, is either associated with the ENSO phenomenon or forced stochastically by the atmosphere. A dipole mode independent of ENSO and originating from air-sea interactions over the Indian Ocean seems not to exist.

Acknowledgments

We would like to thank Dr. D. Dommenget for helpful discussions and suggestions and Dr. S. Legutke, MPIM, Hamburg, for supplying the model data. A. Baquero-Bernal is supported by the "Francisco José de Caldas Institute for the Development of Science and Technology (COLCIENCIAS)", under its scholarships program. Support is also given by the European Union's PROMISE project and by the German Government through its Ocean CLIVAR project.

References

Chambers, D.P., B. D. Tapley, and R. H. Stewart, 1999. Anomalous warming in the Indian Ocean coincident with El Niño. J. Geophys. Res., 99, 7991- 8014.

Dommenget D. and M. Latif, 2001. A cautionary note on the interpretation of EOFs. J. Climate, submitted.

Folland, C. K., D. Parker, A. Colman and R. Washington, 1999. Large scale modes of ocean surface temperature since the late nineteenth century, pp. 73-102 in Beyond El Niño: decadal and interdecadal climate variability, edited by A. Navarra. Springer-Verlag, Berlin.

Hasselmann, K. 1988. PIPs and POPs: the reduction of complex dynamical systems using principal interaction and oscillation patterns. Journal Geophys. Res., 93, 11015-11021.

Hastenrath, S., A. Nicklis, and L. Greischar, 1993. Atmospheric- hydrospheric mechanisms of climate anomalies in the western equatorial Indian Ocean. J. Geophys. Res., 98 (C11), 20 219-20 235.

Latif, M and T. P. Barnett, 1995. Interactions of the tropical Oceans. J. Climate, 8, 952-964.

Legutke, S. and R. Voss, 1999. The Hamburg atmosphere-ocean coupled circulation model ECHO-G. Technical Report 18, German Climate Computer Center (DKRZ).

Meyers, G., 1996. Variation of Indonesian throughflow and El Niño - Southern Oscillation. J. Geophys. Res., 101 (C5), 12 255-12 263.

Murtugudde, R., and A. Busalacchi, 1999. Interannual variability of the dynamics and thermodynamics of the tropical Indian Ocean. J. Climate, 12, 2300-2326.

Reverdin, G., D. Cadet, and D. Gutzler, 1986. Interannual displacements of convection and surface circulation over the equatorial Indian Ocean. Quart. J. Roy. Meteor. Soc., 112, 43-67.

Saji, N. H., B. N. Goswami, P. N. Vinayachandran, and T. Yamagata, 1999. A dipole mode in the Indian Ocean. Nature, 401, 360-363.

Tourre, Y. M. and W. B. White, 1997. Evolution of ENSO signals over the Indo-Pacific domain. J. Phys. Oceanogr., 27, 683-696.

Venzke, S., M. Latif, and A. Villwock, 2000. The coupled GCM ECHO-2, part II: Indian Ocean response to ENSO. J. Climate, in press.

von Storch, H., T. Bruns, I. Fischer- Bruns, and K. Hasselmann, 1988. Principal Oscillation Pattern analysis of the 30-60 day oscillation in a GCM equatorial troposphere. J. Geophys. Res., 93, 11 022-11 036.

Webster, P. J., A. M. Moore, J. P. Loschnigg, and R. R. Leben, 1999. Coupled ocean-atmosphere dynamics in the Indian Ocean during 1997-1998. Nature, 401, 356-360.

Xu, J. S. and H. von Storch, 1990. Principal Oscillation Pattern - prediction of the state of ENSO, J. Climate, 3, 1316-1329.

All seasons:

a) Observations, correlation with western box

b) Observations, correlation with eastern box

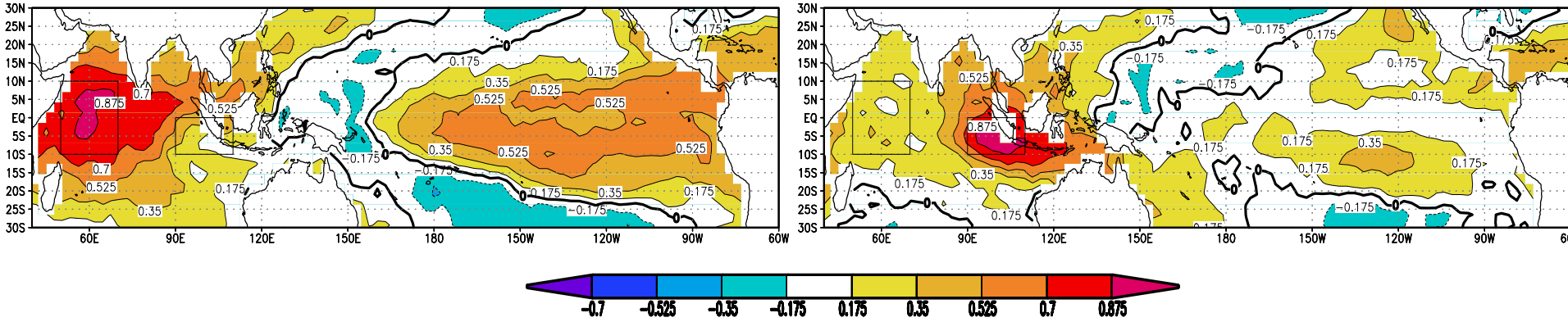

Figure 1: Correlation of a) WTIO box-averaged SST anomalies, and b) SETIO box-averaged SST anomalies with Indo-Pacific SST anomalies for all seasons. SST anomalies from the Hadley Center observational dataset, 1949-1998.

Boreal fall season (SON):

a) Observations, correlation with western box

b) Observations, correlation with eastern box

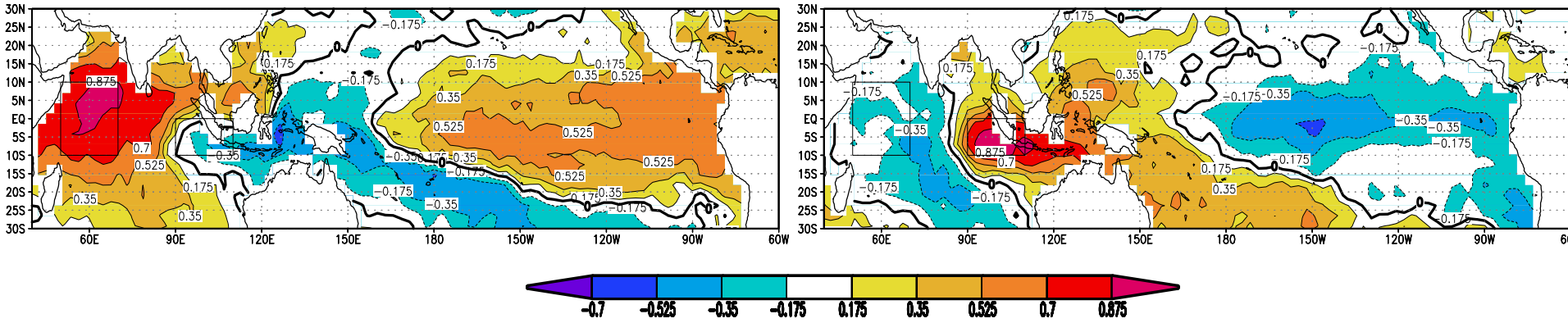

Figure 2: Correlation of a) WTIO box-averaged SST anomalies, and b) SETIO box-averaged SST anomalies with Indo-Pacific SST anomalies for SON. SST anomalies from the Hadley Center observational dataset, 1949- 1998.

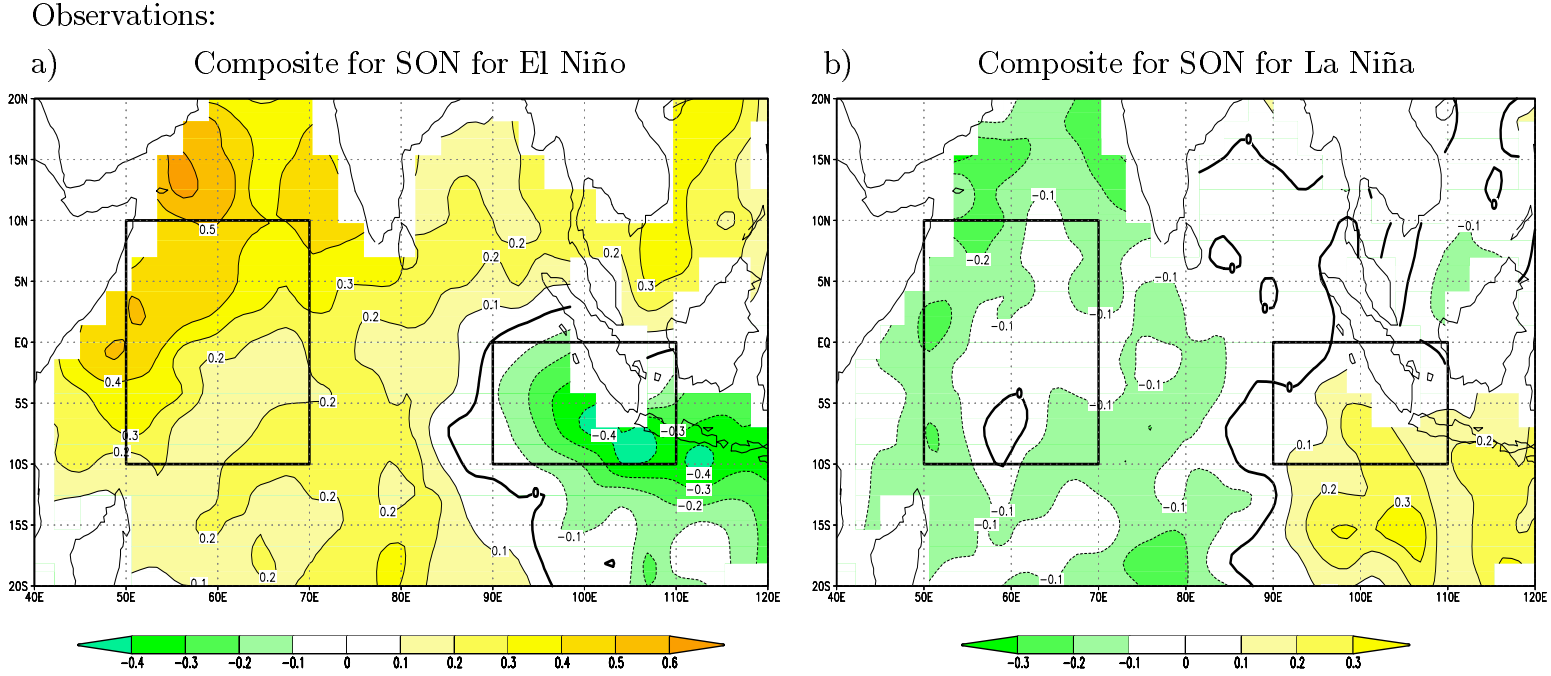

Figure 3: Composites for SON for El Niño and La Niña events. a) Composite of the SST anomalies in SON for the six recent El Niño events. b) Composite of the SST anomalies in SON for the seven recent La Niña events. Units are given in °C.

ENSO signal removed /all seasons:

a) Observations, correlation with western box

b) Observations, correlation with eastern box

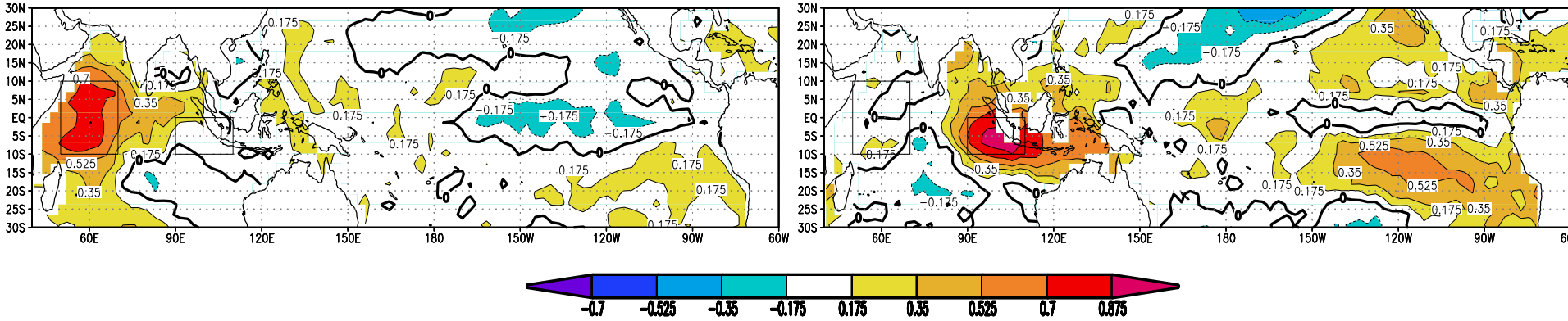

Figure 4: Correlation of a) WTIO box-averaged SST anomalies, and b) SETIO box-averaged SST anomalies with Indo-Pacific SST anomalies for all seasons. SST anomalies from the Hadley Center observational dataset, 1949-1998. ENSO signal was subtracted.

ENSO signal removed /boreal fall season (SON):

a) Observations, correlation with western box

b) Observations, correlation with eastern box

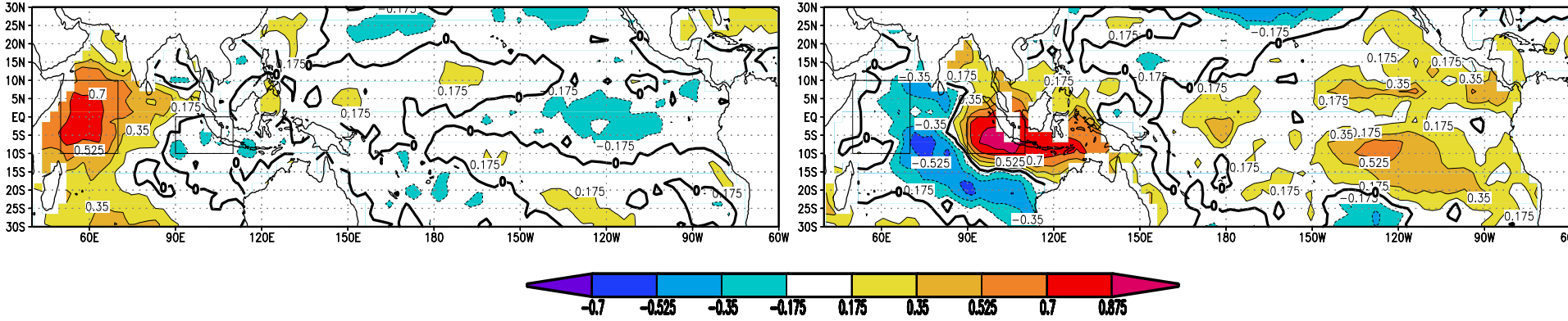

Figure 5: orrelation of a) WTIO box-averaged SST anomalies, and b) SETIO box-averaged SST anomalies with Indo-Pacific SST anomalies for SON. SST anomalies from the Hadley Center observational dataset, 1949- 1998. The ENSO signal was subtracted prior to the analysis.

All seasons:

a)

Control run, correlation with western box

b)

Control run, correlation with eastern box

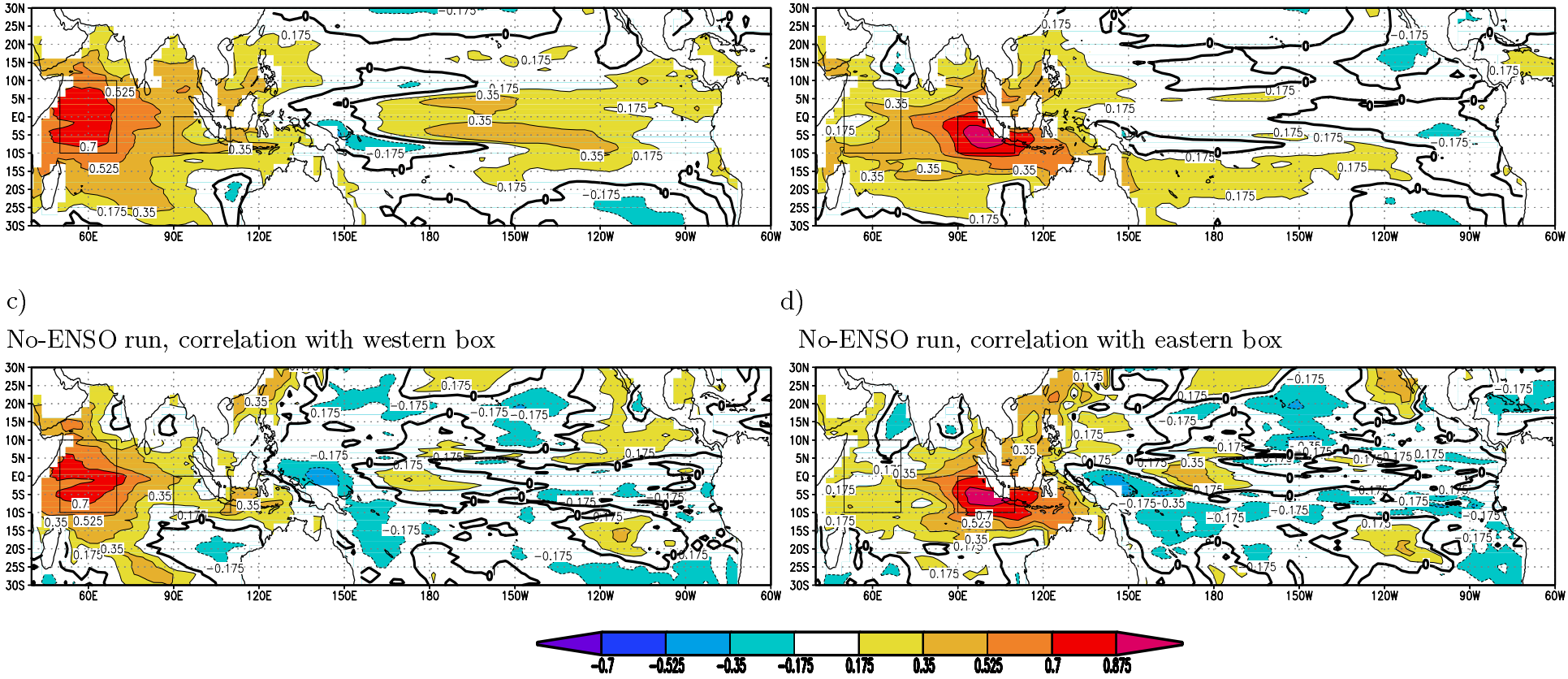

c)

No-ENSO run, correlation with western box

d)

No-ENSO run, correlation with eastern box

Figure 6: Correlation of WTIO box-averaged SST anomalies, SETIO box-averaged SST anomalies with Indo-Pacific SST anomalies for all seasons. a) and b) for SST anomalies from the control run of the CGCM ECHO-G. c) and d) for SST anomalies from the no-ENSO run. In a) and c) correlations are with respect to the WTIO. In b) and d) correlations are with respect to SETIO.

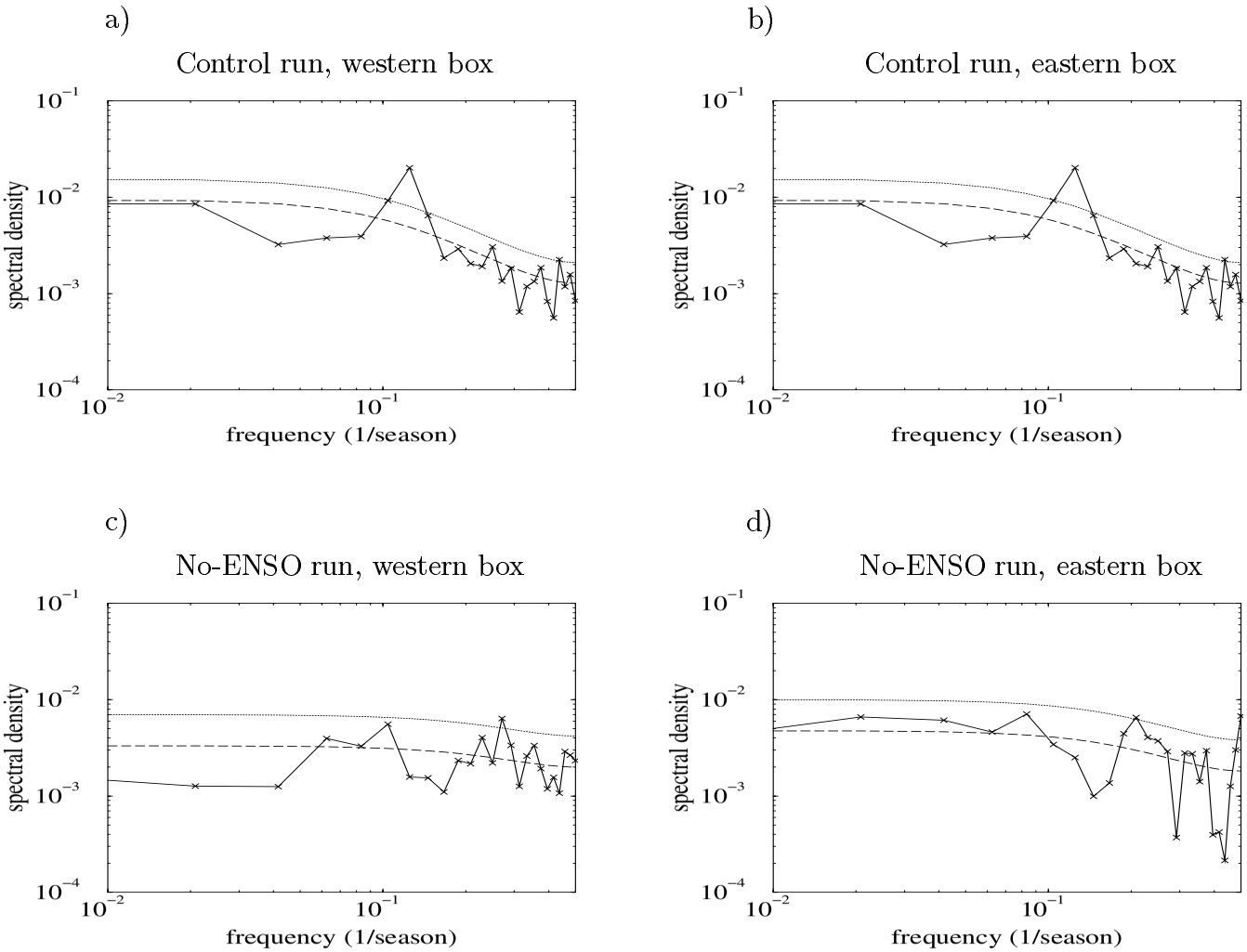

Figure 7: Spectra of box-averaged SST anomalies in the SETIO and WTIO regions when all the seasons are considered. a) and b) for SST anomalies from the control run with the CGCM ECHO-G. c) and d) for SST anomalies from the no-ENSO run. In a) and c) spectra are for WTIO. In b) and d) spectra are for SETIO.

Boreal fall season (SON):

a)

Control run, correlation with western box

b)

Control run, correlation with eastern box

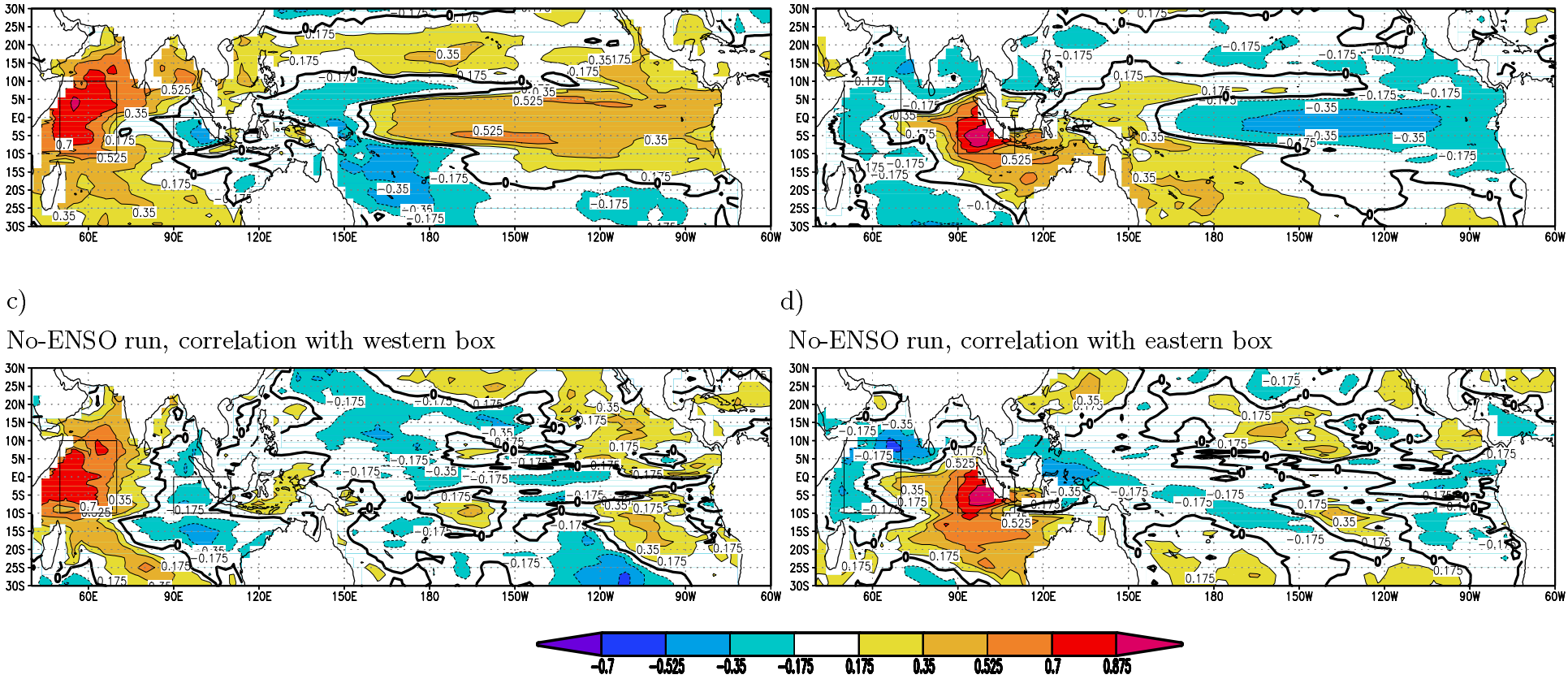

c)

No-ENSO run, correlation with western box

d)

No-ENSO run, correlation with eastern box

Figure 8: Correlation of WTIO box-averaged SST anomalies, SETIO box-averaged SST anomalies with Indo-Pacific SST anomalies for SON. a) and b) are for SST anomalies from the control run of the CGCM ECHO-G. c) and d) for SST anomalies from the no-ENSO run. In a) and c) correlations are with respect to the WTIO. In b) and d) correlations are with respect to SETIO.

All seasons:

a) ECHAM4/mixed layer, correlation with western box

b) ECHAM4/mixed layer, correlation with eastern box

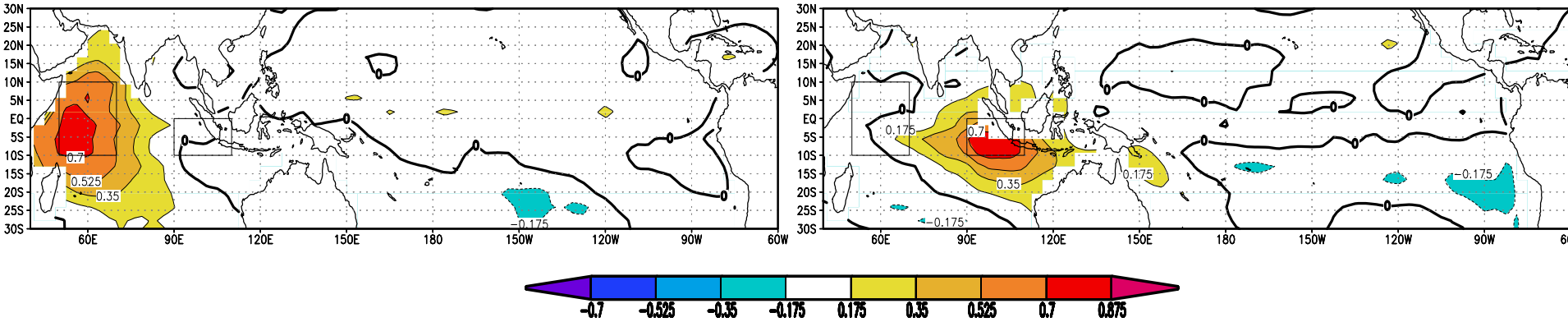

Figure 9: Correlation of a) WTIO box-averaged SST anomalies, and b) SETIO box-averaged SST anomalies with Indo-Pacific SST anomalies for all seasons. The SST anomalies are from the ECHAM4/mixed layer ocean simulation.

Boreal fall season (SON):

a) ECHAM4/mixed layer, correlation with western box

b) ECHAM4/mixed layer, correlation with eastern box

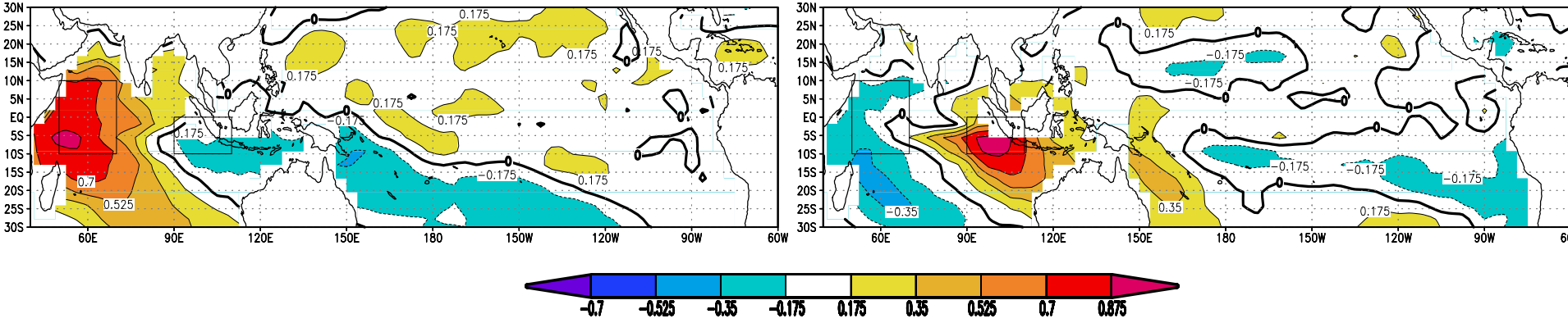

Figure 10: Correlation of a) WTIO box-averaged SST anomalies, and b) SETIO box-averaged SST anomalies with Indo-Pacific SST anomalies for SON. SST anomalies are from the ECHAM4/mixed layer ocean simulation.

MPI-Report-Reference: *Reprinted in

Report 1-276 Please order the reference list from MPI for Meteorology, Hamburg

---

Report No. 277
September 1998

Interannual to Decadal Variability in the Tropical Atlantic
Dietmar Dommenget, Mojib Latif
* Journal of Climate, 1998 (submitted)

Report No. 278
October 1998

Application of a grid-scale lateral discharge model in the BALTEX region
Stefan Hagemann, Lydia Dümenil
* Nordic Hydrology, 30 (3), 209-230, 1999

Report No. 279
October 1998

Cyclostationary Circulation Estimation with a Global Ocean Assimilation System
Detlev Müller, Ralf Giering, Uwe Mikolajewicz, Ernst Maier-Reimer

Report No. 280
October 1998

A coarse grid three dimensional global inverse model of the atmospheric transport
1. Adjoint Model and Jacobian Matrix
2. Inversion of the transport of CO_2 in the 1980s
Thomas Kaminski, Martin Heimann, Ralf Giering
* Journal of Geophysical Research, 1998 (submitted)

Report No. 281
November 1998

Paleonutrient Data Analysis of the Glacial Atlantic using an Adjoint Ocean General Circulation Model
Arne M. E. Winguth, David Archer, Ernst Maier-Reimer, Uwe Mikolajewicz
* AGU Geophysical Monograph Series, Vol. 114, 171-183, 1999

Report No. 282
November 1998

The Effect of Environmental Conditions on Volcanic Plume Rise
Hans-F. Graf, Michael Herzog, Josef M. Oberhuber, Christiane Textor
* Journal of Geophysical Research, 1998 (submitted)

Report No. 283
December 1998

Model Simulations of the Changing Distribution of Ozone and its Radiative Forcing of Climate:
Past, Present and Future
Geert-Jan Roelofs, Jos Lelieveld, Johann Feichter

Report No. 284
December 1998

Predicting the Number of Cloud Droplets in the ECHAM GCM
Ulrike Lohmann, Johann Feichter, Catherine C. Chuang, Joyce E. Penner
* Journal of Geophysical Research - Atmospheres, 1998 (accepted)

Report No. 285
December 1998

The Role of Ocean Dynamics for Low-Frequency Fluctuations of the NAO in a Coupled Ocean-Atmosphere GCM
Michael Christoph, Uwe Ulbrich, Josef M. Oberhuber, Erich Roeckner

Report No. 286
January 1999

Formation of nitrous acid: Parameterisation and comparison with observations
Gerhard Lammel

Report No. 287
Februar 1999

Natürliche Senken und Quellen des atmosphärischen Kohlendioxids: Stand des Wissens und Optionen des Handelns
Martin Heimann, Christine Weber, Jan C. Duinker, Arne Körtzinger, Ludger Mintrop, Nina Buchmann, Ernst-Detlef Schulze, Michaela Hein, Alberte Bondeau, Wolfgang Cramer, Marcus Lindner, Gerd Esser

Report No. 288
March 1999

Large-eddy simulation of a nocturnal stratocumulus-topped marine atmospheric boundary layer:
An uncertainty analysis
Andreas Chlond, Andreas Wolkau
Boundary-Layer Meteorology, 95,31-55, 2000

Report No. 289
March 1999

Derivation of global GCM boundary conditions from 1 km land use satellite data
Stefan Hagemann, Michael Botzet, Lydia Dümenil, Bennert Machenhauer

Report No. 290
June 1999
A nonlinear impulse response model of the coupled carbon cycle-ocean-atmosphere climate system
Georg Hooss, Reinhard Voss, Klaus Hasselmann, Ernst Maier-Reimer, Fortunat Joos

Report No. 291
June 1999
Rapid algorithms for plane-parallel radiative transfer calculations
Vassili Prigarin

Report No. 292
June 1999
Oceanic Control of Decadal North Atlantic Sea Level Pressure Variability in Winter
Mojib Latif, Klaus Arpe, Erich Roeckner
* Geophysical Research Letters, 1999 (submitted)

Report No. 293
July 1999
A process-based, climate-sensitive model to derive methane emissions from natural wetlands: Application to 5 wetland sites, sensitivity to model parameters and climate
Bernadette P. Walter, Martin Heimann
* Global Biogeochemical Cycles, 1999 (submitted)

Report No. 294
August 1999
Possible Changes of $\delta^{18}O$ in Precipitation Caused by a Meltwater Event in the North Atlantic
Martin Werner, Uwe Mikolajewicz, Georg Hoffmann, Martin Heimann
* Journal of Geophysical Research - Atmospheres, 105, D8, 10161-10167, 2000

Report No. 295
August 1999
Borehole versus Isotope Temperatures on Greenland: Seasonality Does Matter
Martin Werner, Uwe Mikolajewicz, Martin Heimann, Georg Hoffmann
* Geophysical Research Letters, 27, 5, 723-726, 2000

Report No. 296
August 1999
Numerical Modelling of Regional Scale Transport and Photochemistry directly together with Meteorological Processes
Bärbel Langmann
* Atmospheric Environment, 34, 3585-3598, 2000

Report No. 297
August 1999
The impact of two different land-surface coupling techniques in a single column version of the ECHAM4 atmospheric model
Jan-Peter Schulz, Lydia Dümenil, Jan Polcher
* Journal of Applied Meteorology, 40, 642-663, 2001

Report No. 298
September 1999
Long-term climate changes due to increased CO_2 concentration in the coupled atmosphere-ocean general circulation model ECHAM3/LSG
Reinhard Voss, Uwe Mikolajewicz
* Climate Dynamics, 17, 45-60, 2001

Report No. 299
October 1999
Tropical Stabilisation of the Thermohaline Circulation in a Greenhouse Warming Simulation
Mojib Latif, Erich Roeckner
* Journal of Climate, 1999 (submitted)

Report No. 300
October 1999
Impact of Global Warming on the Asian Winter Monsoon in a Coupled GCM
Zeng-Zhen Hu, Lennart Bengtsson, Klaus Arpe
* Journal of Geophysical Research-Atmosphere, 105, D4, 4607-4624, 2000

Report No. 301
December 1999
Impacts of Deforestation and Afforestation in the Mediterranean Region as Simulated by the MPI Atmospheric GCM
Lydia Dümenil Gates, Stefan Ließ

Report No. 302
December 1999
Dynamical and Cloud-Radiation Feedbacks in El Niño and Greenhouse Warming
Fei-Fei Jin, Zeng-Zhen Hu, Mojib Latif, Lennart Bengtsson, Erich Roeckner
* Geophysical Research Letter, 28, 8, 1539-1542, 2001

Report No. 303
December 1999
The leading variability mode of the coupled troposphere-stratosphere winter circulation in different climate regimes
Judith Perlwitz, Hans-F. Graf, Reinhard Voss
* Journal of Geophysical Research, 105, 6915-6926, 2000

Report No. 304
January 2000
Generation of SST anomalies in the midlatitudes
Dietmar Dommenget, Mojib Latif
* Journal of Climate, 1999 (submitted)

Report No. 305
June 2000
Tropical Pacific/Atlantic Ocean Interactions at Multi-Decadal Time Scales
Mojib Latif
* Geophysical Research Letters, 28,3,539-542,2001

Report No. 306
June 2000
On the Interpretation of Climate Change in the Tropical Pacific
Mojib Latif
* Journal of Climate, 2000 (submitted)

Report No. 307
June 2000
Observed historical discharge data from major rivers for climate model validation
Lydia Dümenil Gates, Stefan Hagemann, Claudia Golz

Report No. 308
July 2000
Atmospheric Correction of Colour Images
of Case I Waters - a Review
of Case II Waters - a Review
D. Pozdnyakov, S. Bakan, H. Grassl
* Remote Sensing of Environment, 2000 (submitted)

Report No. 309
August 2000
A Cautionary Note on the Interpretation of EOFs
Dietmar Dommenget, Mojib Latif
* Journal of Climate, 2000 (submitted)

Report No. 310
September 2000
Midlatitude Forcing Mechanisms for Glacier Mass Balance Investigated Using General Circulation Models
Bernhard K. Reichert, Lennart Bengtsson, Johannes Oerlemans
* Journal of Climate, 2000 (accepted)

Report No. 311
October 2000
The impact of a downslope water-transport parameterization in a global ocean general circulation model
Stephanie Legutke, Ernst Maier-Reimer

Report No. 312
November 2000
The Hamburg Ocean-Atmosphere Parameters and Fluxes from Satellite Data (HOAPS):
A Climatological Atlas of Satellite-Derived Air-Sea-Interaction Parameters over the Oceans
Hartmut Graßl, Volker Jost, Ramesh Kumar, Jörg Schulz, Peter Bauer, Peter Schlüssel

Report No. 313
December 2000
Secular trends in daily precipitation characteristics: greenhouse gas simulation with a coupled AOGCM
Vladimir Semenov, Lennart Bengtsson

Report No. 314
December 2000
Estimation of the error due to operator splitting for micro-physical-multiphase chemical systems in meso-scale air quality models
Frank Müller
* Atmospheric Environment, 2000 (submitted)

Report No. 315
January 2001
Sensitivity of global climate to the detrimental impact of smoke on rain clouds
Hans-F. Graf, Daniel Rosenfeld, Frank J. Nober
* nur unter www.mpimet.mpg.de · Veröffentlichungen · MPI-Reports

Report No. 316 March 2001	**Lake Parameterization for Climate Models** Ben-Jei Tsuang, Chia-Ying Tu, Klaus Arpe
Report No 317 March 2001	**The German Aerosol Lidar Network:** **Methodology, Data, Analysis** J. Bösenberg, M. Alpers, D. Althausen, A. Ansmann, C. Böckmann, R. Eixmann, A. Franke, V. Freudenthaler, H. Giehl, H. Jäger, S. Kreipl, H. Linné, V. Matthias, I. Mattis, D. Müller, J. Sarközi, L. Schneidenbach, J. Schneider, T. Trickl, E. Vorobieva, U. Wandinger, M. Wiegner
Report No. 318 March 2001	**On North Pacific Climate Variability** Mojib Latif * Journal of Climate, 2001 (submitted)
Report No. 319 March 2001	**The Madden-Julian Oscillation in the ECHAM4 / OPYC3 CGCM** Stefan Liess, Lennart Bengtsson, Klaus Arpe * Climate Dynamics, 2001 (submitted)
Report No. 320 May 2001	**Simulated Warm Polar Currents during the Middle Permian** A. M. E. Winguth, C. Heinze, J. E. Kutzbach, E. Maier-Reimer, U. Mikolajewicz, D. Rowley, A. Rees, A. M. Ziegler * Paleoceanography, 2001 (submitted)
Report No. 321 June 2001	**Impact of the Vertical Resolution on the Transport of Passive Tracers in the ECHAM4 Model** Christine Land, Johann Feichter, Robert Sausen * Tellus, 2001 (submitted)
Report No.322 August 2001	**Summer Session 2000** **Beyond Kyoto: Achieving Sustainable Development** Edited by Hartmut Graßl and Jacques Léonardi
Report No.323 July 2001	**An atlas of surface fluxes based on the ECMWF Re-Analysis- a climatological dataset to force global ocean general circulation models** Frank Röske
Report No.324 August 2001	**Long-range transport and multimedia partitioning of semivolatile organic compounds:** **A case study on two modern agrochemicals** Gerhard Lammel, Johann Feichter, Adrian Leip * Journal of Geophysical Research-Atmospheres, 2001 (submitted)
Report No. 325 August 2001	**A High Resolution AGCM Study of the El Niño Impact on the North Atlantic / European Sector** Ute Merkel, Mojib Latif * Geophysical Research Letters, 2001 (submitted)
Report No. 326 August 2001	**On dipole-like variability in the tropical Indian Ocean** Astrid Baquero-Bernal, Mojib Latif * Journal of Climate, 2001 (submitted)

ISSN 0937-1060